FISEVIER

Contents lists available at SciVerse ScienceDirect

Journal of Membrane Science

journal homepage: www.elsevier.com/locate/memsci



Towards direct potable reuse with forward osmosis: Technical assessment of long-term process performance at the pilot scale



Nathan T. Hancock ^a, Pei Xu ^a, Molly J. Roby ^a, Juan D. Gomez ^b, Tzahi Y. Cath ^{a,*}

- ^a Department of Civil and Environmental Engineering, 1500 Illinois Street, Colorado School of Mines, Golden, CO 80401, USA
- ^b CH2M Hill, 9311 San Pedro Avenue, San Antonio, TX 78216, USA

ARTICLE INFO

Article history: Received 28 November 2012 Received in revised form 14 April 2013 Accepted 26 April 2013 Available online 23 May 2013

Keywords:
Forward osmosis
Osmotic dilution
Reverse osmosis
Water reuse
Membrane fouling
Seawater desalination

ABSTRACT

In this study we evaluated the performance of forward osmosis (FO) at the pilot scale to achieve simultaneous seawater desalination and wastewater reclamation. The investigation was performed with a commercial spiral wound FO membrane element for approximately 1300 h of continuous operation, processing 900,000 L of wastewater effluent and producing 10,000 L of purified water through a hybrid FO-RO process. Water and solute fluxes were monitored during the study. Reversible and irreversible membrane fouling was observed; however, water flux was maintained at a relatively constant rate of 5.7 + 0.2 L m⁻² h⁻¹ with MBR permeate feed and seawater draw solution. Subsequent increase of total suspended solids (TSS) concentration in the FO feed (secondary treated effluent with 5 to 16 mg L⁻¹ TSS) resulted in incremental flux decline; however, the membrane typically achieved stable water flux after the initial exposure to foulants. Additional analysis focused on bi-directional transport of inorganic species and a detailed evaluation of dissolved organic matter permeation through the membranes in the hybrid process. Evaluation of sample fluorescence revealed that the FO membrane and the hybrid process provide a strong barrier to protein-like fluorophores associated with wastewater effluent. Results also demonstrated the robust nature of dual barrier membrane systems to achieve greater than 99.9% removal of orthophosphate and dissolved organic carbon and more than 96% rejection of nitrate. Upon completion of the study a comprehensive membrane autopsy was performed on the FO and RO membranes. Organic fouling on the FO membrane was observed to have low adhesion to the membrane surface, but did result in some modification to membrane active layer properties.

© 2013 Elsevier B.V. All rights reserved.

1. Introduction

Novel water treatment technologies and new process configurations can facilitate more effective treatment of unconventional water sources and expand the reuse of reclaimed water, ultimately achieving direct potable reuse [1,2]. One emerging class of water treatment technologies is osmotically driven membrane processes (ODMPs). These technologies rely on osmotic pressure difference across a semipermeable membranes, induced by a hypertonic draw solution (DS) rather than by hydraulic pressure or thermal evaporation, to achieve separation of dissolved constituents from a feed stream [3]. Many previous studies focused on forward osmosis (FO) (e.g., closed-loop reconcentration of the draw

* Corresponding author. Tel.: +1 303 273 3402. E-mail address: tcath@mines.edu (T.Y. Cath). solution) and were conducted at the bench-scale [4]. These studies highlighted the apparent benefits of the FO process to treat highly impaired water without incurring substantial irreversible membrane fouling. While a few studies [5–8] explored the capability of FO systems to achieve separations of dissolved constituents with reduced energy demand in specific treatment scenarios, others [9] observed that the FO process may not be energy efficient in general applications because the energy required to reconcentrate a draw solution in a closed-loop process with reverse osmosis (RO) is too high.

Like FO, osmotic dilution (ODN) is an ODMP that can be used to simultaneously facilitate water reclamation [10–12] and wastewater concentration [13]; yet, ODN is also capable of simultaneously reducing the energy consumption during desalination while providing additional process intensification [10,11,14]. The ODN process employs seawater or other readily available brines as DS to extract water from a co-located source of impaired water. When the DS (e.g., seawater) is diluted, and its osmotic pressure declines, it can lower the hydraulic pressure required during desalination and production of purified water with RO. Recent bench-scale studies [10,11,14–16] of ODN evaluated the different

Abbreviations: DOC, Dissolved organic carbon; DS, Draw solution; EDS, Energy dispersive spectroscopy; EEM, Excitation-emission matrix; FO, Forward osmosis; MBR, Membrane bioreactor; ODN, Osmotic dilution; RO, Reverse osmosis; SBMBR, sequencing batch membrane bioreactor; SUVA, Specific ultraviolet absorbance; TDS, Total dissolved solids; TOC, Total organic carbon; TSS, Total suspended solids.

aspects of synergistically performing water reclamation and seawater desalination.

Bench-scale investigation during our recent study [10] revealed that water flux during ODN was minimally affected by variable feed water quality (i.e., deionized water, secondary and tertiary treated effluent, and surface water impacted by effluent). Specific reverse salt flux (i.e., the ratio of DS solute (sea salts) flux into the feed and water flux into the DS [17]) varied between 400 and 650 mg TDS per liter of water recovered from the feed. It was also demonstrated that membrane fouling under specific flow conditions could be substantially reduced and constant water flux could be maintained. Results from the investigation illustrated that water flux decline due to membrane fouling was partially reversible with physical cleaning of the FO membrane, and that moderate chemical cleaning was able to fully recover water flux. Other recent studies [11,18,19] confirmed this observation, and two previous studies [10,11] also identified favorable economic return on investment and indicated cost efficiency of the ODN process compared to conventional high pressure seawater desalination.

A recent life cycle assessment study [14] also compared ODN to several established desalination and wastewater reclamation technologies from an environmental impact and energy efficiency perspective. This study identified several currently achievable modifications to FO membranes, their packaging, and system design and operation that can achieve favorable reductions in environmental impact relative to other established technologies for desalination and water reclamation. Yet, limitations associated with non-standard membrane components, site logistics, control system sophistication, and organic and trace organic compound analytical methods during our initial study [10] presented several opportunities to further explore the performance and efficiency of the ODN process. An additional limitation of recent studies [10,11] is that the FO membrane cells employed were not optimized for commercial applications.

The main objectives of this study were to investigate, at a pilot scale, the performance of future ODN process in a dual barrier FO-RO configuration and the robustness of a commercial spiral wound FO membrane. Long-term water flux, fouling resistance and flux recovery, and permeation of dissolved organic matter and inorganic compounds were evaluated during more than 1200 h of continuous operation with municipal wastewater feed of varying quality. A comprehensive membrane autopsy was performed at the conclusion of the study. Simultaneously, we have investigated transport of trace organic compounds (TOrCs) through the dual barrier process, also at the pilot scale [16]. These results, in addition to other recent complimentary studies [20-22], provide confirmation of the efficacy of FO hybrid processes for treatment of TOrCs. To achieve these objectives, the spiral wound FO membrane element was integrated with an RO pilot system to form an FO-RO hybrid process that simulates the envisioned ODN process.

2. Material and methods

2.1. Pilot-scale system design

The pilot scale FO–RO hybrid system was deployed at the Mines Park wastewater treatment research facility located on the campus of the Colorado School of Mines student-housing complex. 7200 gallons of municipal wastewater are treated at the facility every day by a demonstration scale sequencing batch membrane bioreactor (SBMBR) system [23].

Although ODN was the focus of this investigation, experiments were conducted in FO mode (i.e., closed loop DS configuration)

because a continuous supply of seawater was not available at the testing site; therefore, the term FO is used throughout this manuscript. Under these conditions, accumulation of constituents that diffuse from the feed into the closed loop DS is inevitable and imposes a greater challenge to the hybrid process. The dual barrier characteristics of the hybrid process will be further enhanced in coastal settings where a seawater DS flows in a once-through pattern.

A flow diagram of the pilot-scale hybrid process is illustrated in Fig. 1. A high-pressure, variable speed, positive displacement pump (HydraCell M03, Wanner Engineering Inc., Minneapolis, MN) was utilized to pressurize the diluted DS into a 1-1-1 array of three RO membrane elements. Permeate from the first RO membrane was collected in the product water tank while the combined permeate from the second and third membranes were returned to the RO feed tank. The concentrate from the third RO membrane was used as the DS for the FO process.

The spiral wound FO membrane element was installed vertically on the frame of the RO subsystem. In the spiral wound FO element, DS from the RO subsystem is pumped into the DS inlet at the bottom of the element using residual pressure from the RO concentrate. The DS then flows into the core tube where it is diverted into the membrane envelope as shown in previous publications [16,24,25]. Diluted DS exits the membrane from the core tube outlet located at the top of the FO membrane element and flows back to the RO feed tank. Installing the element vertically and allowing the DS to flow upwards ensured venting of entrained air from the membrane envelope.

A constant speed rotary vane pump (Procon, Murfreesboro, TN) supplies a continuous flow of impaired feed water to the feed inlet at the top of the FO membrane element. The feed stream flows down through the element, tangential to the active layer of the FO membrane, and exits the membrane through an outlet at the

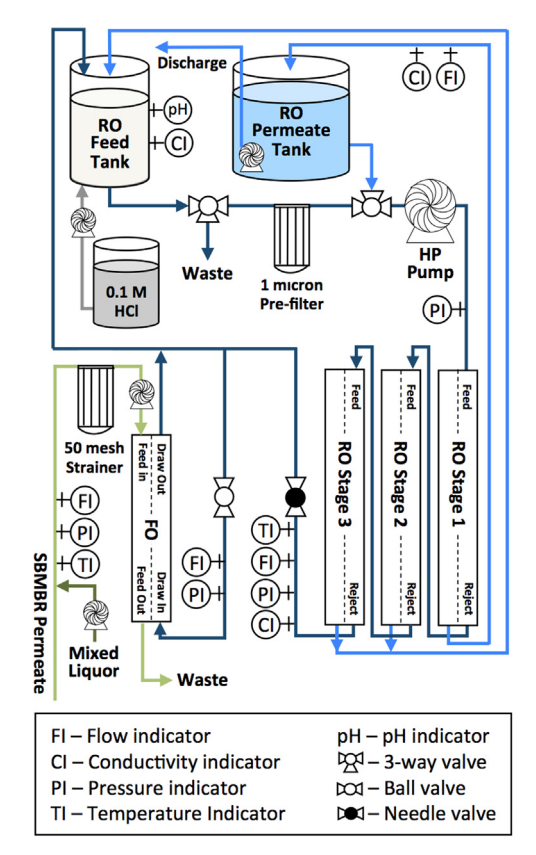


Fig. 1. Schematic of the hybrid FO–RO process for simultaneous wastewater reclamation and seawater desalination.

bottom of the element. This flow configuration allows easy and continuous flushing of suspended solids out of the membrane element

2.2. Membranes

Three commercial seawater RO spiral wound membranes (SW30 2540, DOW Filmtec, Edina, MN) were used in the RO pilot system. A spiral wound (standard size 4 in. diameter/40 in. long) FO membrane element was acquired from Hydration Technology Innovations (HTI) (Albany, OR). The membrane is thought to incorporate a cellulose triacetate (CTA) active layer cast directly onto a woven polyester mesh [26].

The novel spiral wound FO element was made of a single membrane envelope with an active area of 1.58 m² and it was installed inside a conventional 4040 pressure vessel. This spiral wound membrane element uses a more open feed spacer than those commonly employed in spiral wound RO membranes. The corrugated feed spacer provides larger and more continuous channels for fluid flow to accommodate suspended solids and other debris that might be present in impaired feed water.

Water permeance and NaCl rejection for the virgin CTA membrane were measured during experiments conducted in RO mode with a SEPA-CF membrane test cell (Sterlitech Corporation, Kent, WA) [27]. Feed at a constant temperature of 25 °C was either deionized water for permeance tests or a 2000 mg L $^{-1}$ NaCl solution for rejection tests. Tests were conducted with feed pressures of 6.9 and 10.3 bar (100 and 150 psig). Water permeance and NaCl rejection for the SW30 membrane were obtained from the manufacturers technical specifications data sheet [28]. Both FO and RO membrane parameters are summarized in Table 1.

2.3. System PLC development and capabilities

System control and data recording were managed by a programmable logic control (PLC) system specifically designed for this study. The electronic transmitters and analog gages used in the system are also illustrated in Fig. 1. Active controls were programmed to maintain constant and predetermined DS concentration, drain the RO product water tank, dose acid solution (0.1 M HCl) into the DS to maintain a pH of 6, and facilitate emergency shutdown of the system in case operating parameters indicate a system malfunction. All transmitters were connected to a LabJack data acquisition card (UE9-Pro, LabJack Corporation, Lakewood, CO) that communicates with a system control program (LabVIEW 7.0, National Instruments. Austin, TX).

The RO system was designed to produce constant DS concentration while removing water from the DS at approximately the same rate that water permeated through the FO membrane into the DS. However, due to loss of DS solute through both the FO and RO membranes, calculation of water flux through the FO membrane had to take into account both RO permeate flowrate and the slow decline in brine volume in the RO feed tank (overproduction of RO permeate due to loss of salt from the closed loop DS). Thus, FO water flux was calculated by subtracting DS volume loss rate

Table 1Water permeance and NaCl rejection for the FO and RO membranes used in this study.

Membrane	Water permeance ${\rm L}{\rm m}^{-2}{\rm h}^{-1}{\rm bar}^{-1}$	NaCl rejection %		
CTA [26] SW30 [27]	$\begin{array}{c} 0.78 \pm 0.02 \\ 1.31 \end{array}$	$93.2 \pm 0.9^*$ 99.4		

^{*} Value based on flat sheet coupon performance.

from the RO permeate flow rate and dividing by the FO membrane area.

2.4. Pilot-scale system operation

2.4.1. Solution chemistries

Synthetic sea salt (Instant Ocean, Mentor, OH) was used to prepare the DS. The mass fraction of each inorganic constituent in 1 g of synthetic sea salt is summarized in Table 2. SBMBR permeate was the feed to the FO and was continuously pumped into the feed side of the FO spiral wound membrane element at a rate of 12 L/min. The quality of the FO feed water (SBMBR effluent with or without dosing of mixed liquor solids) was subject to change because of the decentralized nature of the SBMBR facility. Average SBMBR permeate water quality based on 23 samples taken over a 38 day period is summarized in Table 3.

Table 2Mass fraction of inorganic constituents in the synthetic sea salt used in this study.

Constituent	Mass fraction %	Constituent	Mass fraction %
Bicarbonate	0.57	Nitrate	0.02
Boron	0.02	O-phosphate	0.01
Barium	< 0.001	Potassium	1.15
Bromide	0.22	Silica	0.001
Calcium	1.26	Sodium	30.5
Chloride	54.8	Strontium	0.03
Magnesium	3.54	Sulfate	8.02

Table 3Average concentrations of major constituents and water quality parameters measured in the SBMBR permeate.

Constituent	Concentration, $\operatorname{mg} \operatorname{L}^{-1}$	Constituent	Concentration, $\operatorname{mg} \operatorname{L}^{-1}$
Bicarbonate	54.3 ± 1.7	O-phosphate	12.3 ± 2.5
Boron	0.08 ± 0.04	Potassium	11.7 ± 1.7
Barium	0.06 ± 0.02	pН	7.1 ± 0.1
Bromide	0.06 ± 0.01	Silica	10.6 ± 1.1
Calcium	36.1 ± 3.6	Sodium	54.5 ± 3.6
Chloride	72.0 ± 5.6	Strontium	0.20 ± 0.02
DOC	3.9 ± 0.7	Sulfate	79.8 ± 5.4
Magnesium	10.3 ± 1.0	SUVA,	2.4 ± 0.1
		$L mg^{-1} m^{-1}$	
Nitrate	37.3 ± 15.4	TDS	325.0 ± 22.7

Table 4Summary of operating conditions during the pilot study. Letter indices represent unique intervals during the operation of the pilot system.

Hours of operation	DS conc. mg L ⁻¹	DS flow rate L min ⁻¹	Feed TSS conc. $\rm mg~L^{-1}$	FO feed pressure psig
0-350 (A)	$30,000 \pm 600$	1.6 ± 0.3	0	0
350-500 (B) ^a	$54,\!490 \pm 1340$	2.0 ± 0.3	0	0
530-650 (C) ^a	$27,550 \pm 300$	2.3 ± 0.2	0	0
650-740 (D)	$29,520 \pm 350$	2.2 ± 0.1	5.3 ± 1.6	0
740-890 (D)b	$28,660 \pm 1240$	2.4 ± 0.3	15.9 ± 2.0	0
890-940 (E)b	$29,590 \pm 1340$	2.3 ± 0.1	50.2 ± 6.3	0
940-1180 (F)	$29,590 \pm 1340$	2.3 ± 0.1	16.4 ± 2.8	0
1200-1250 (G)	$29,590 \pm 1340$	2.3 ± 0.1	16.4 ± 2.8	10
1270–1320 (G)	$29,590 \pm 1340$	1.9 ± 0.2	16.4 ± 2.8	20

^a Chemical cleaning of the RO subsystem performed between intervals B and C.

^b Feed flow reversal performed on FO spiral wound membrane for one hour prior to increasing TSS concentration during interval E.

2.4.2. Operating conditions

Operating conditions during the study are listed in Table 4. The pilot-scale system was initially tested for 27 days with SBMBR permeate. Thereafter, the FO feed was constantly dosed with biosolids from the SBMBR mixed liquor to simulate secondary effluent by targeting different concentrations of total suspended solids (TSS) in the feed stream to the FO membrane. TSS concentration was measured after screening through a 50-mesh strainer. The concentration of DS was increased in interval B to investigate process response to high water flux events, and in interval G pressure was added to the feed side of the FO spiral wound membrane to simulate hydraulic conditions within a multielement pressure vessel. Water flux restoration by physical and chemical cleaning of the membrane was also evaluated. Physical cleaning was achieved with reversal of the feed water flow direction through the membrane element for 1 h. Chemical cleaning was performed by recirculating a liquid acid cleaner and detergent solution (Citranox, Alconox, White Plains, NY) diluted in 100 L of RO permeate to a pH of 4.5 for 15 min.

2.5. Analytical methods

2.5.1. Analytical methods for inorganic constituents

Anion analysis was conducted using an ion chromatograph (IC) (DC80, Dionex, Sunnyvale, CA) according to Standard Method 4110 B [29]. DS and permeate samples were diluted as necessary to bring chloride concentration to below 300 mg $\rm L^{-1}$, and feed samples were filtered through a 0.45 μm polymeric filters to remove suspended solids prior to analysis.

Cation analysis was conducted using inductively coupled plasma atomic emission spectroscopy (ICP-AES) (Optima 3000, Perkin Elmer, Norwalk, CT) according to Standard Method 3120 B [29]. DS and permeate samples were diluted as necessary to bring their sodium concentration below 500 mg $\rm L^{-1}$. ICP samples were acidified with HNO3 to a pH of less than 2. Feed samples were filtered prior to analysis with 0.45 μm polymeric filters to remove suspended solids.

2.5.2. Analytical methods for organic constituents

Several analytical techniques were used to evaluate the character and permeation of organic matter through the two dense membrane barriers. Transport of organic matter through the hybrid process was evaluated and qualified using total dissolved organic carbon (DOC) analysis, spectrum ultraviolet absorbance between 240 and 600 nm, and fluorescence spectroscopy.

TSS was measured according to Standard Method 2540 D [29] using a 1.2 μ m filter. DOC analysis was conducted using a catalytically-aided platinum combustion TOC analyzer (TOC-5000A, Shimadzu Scientific Instruments, Columbia, MD) on samples that were filtered with a 0.45 μ m filter. Additional characterization of DOC was performed with full spectrum UV absorbance (wavelength range between 240 and 600 nm) using a bench-top spectrophotometer (DU 800, Beckman Coulter, Brea, CA) according to Standard Method 5910 B [29]. Full wavelength UVA measurements were used during the processing of fluorescence microscopy data (discussed below). Additionally, the ratio of sample UVA at 254 nm to the DOC concentration (called the specific UVA (SUVA)) was calculated and is used as an indicator of the molecular weight distribution of DOC in a sample [30].

Fluorescence intensity of samples at 20 °C was measured for excitation wavelengths between 240 and 450 nm and emission wavelengths between 290 and 580 nm (in 10 nm increments) with a 3-dimensional spectrofluorometer (FluorMax-4, HORIBA Jobin Yvon Inc., Edison, NJ). Samples were prepared and analyzed according to Cory [31] and Ohno [32]. Fluorophores detected in

specific areas of optical space within an excitation-emission-intensity matrix (EEM) are related to specific fractions of DOC based on information gathered from previous studies [33–36]. Fluorophores were classified in previous studies as peak A (humic acid- and fulvic acid-like material ($\lambda_{\rm ex/em}=237-270/400-500$ nm)), peak C (humic acid-like ($\lambda_{\rm ex/em}=300-370/400-500$ nm)), and peak T_1 (tryptophan and protein-like material related to biological activity ($\lambda_{\rm ex/em}=275-290/340-360$ nm)). Peak A and peak C are associated with humic and fulvic acids occurring in natural organic matter derived from plant material [34]. Peak T_1 is frequently observed in wastewater samples because sewage-derived DOC contains organic matter originating from microbial activity (i.e., soluble microbial products and extracellular biological organic matter [33,35]). Select EEMs was normalized by the corresponding sample DOC concentration to improve DOC differentiation.

2.5.3. Membrane autopsy and characterization methods

The FO and all three RO membranes were removed from the pilot system after 55 days of continuous operation and membrane autopsies were conducted to characterize the fouling and scaling on membranes. Membrane coupons were obtained from the center of the feed and concentrate ends of each RO membrane. Four membrane coupons were obtained from the FO membrane, two from the inlet (one near the central collection tube and one near the outer edge of the membrane envelope) and two from similar locations at the membrane outlet.

Five methods were employed to characterize the active layer of virgin and fouled FO and RO membranes as well as the DS side of the FO membrane. Field emission scanning electron microscopy (FESEM) (ISM-7000F, IEOL, Tokyo, Japan) was used to observe the surface and cross-section of FO and RO membrane. Energy dispersive X-ray spectroscopy (EDS) (EDAX Genesis, JEOL, Tokyo, Japan) was employed during FESEM imaging to provide elemental analysis of deposits identified on membrane surfaces. Surface functional groups of FO and RO membranes were analyzed with a Fourier transform infrared (FTIR) spectrometer (Nicolet 4700 FT-IR, Thermo Electron Corporation, Madison, WI) using the attenuated total reflection (ATR) method. Contact angle measurements were obtained with a goniometer (Model 200-00, Rame-Hart Instrument Company, Netcong, NJ). Measurements were performed at multiple locations on each sample using the captive bubble method [37]. Surface charge (zeta potential) measurements were obtained with an electrokinetic analyzer (SurPass, Anton Paar, Graz, Austria) using an adjustable gap cell. Zeta potential was calculated using the Helmholtz-Smoluchowski evaluation method. Membrane surface charge was characterized using a 2 mM KCl electrolyte solution at a pH range between 4 and 9. Additional membrane biofouling characterization was performed with a fluorescence microscope (Motorized Widefield DMRXA, Leica, Bannockburn, IL) using the SYBR Green staining method.

3. Results and discussion

3.1. Water productivity

3.1.1. Water flux

Water flux was continually monitored during the study. Water flux as a function of operation time is presented in Fig. 2. Letter indices represent operation intervals enumerated in Table 4. During 1300 h (55 days) of continuous operation the hybrid FO–RO process produced approximately 10,000 L of purified water and processed more than 900,000 L of wastewater effluent (FO feed).

During interval A, the system was operated for approximately 250 h with MBR permeate before reaching a steady-state water flux of 5.5 ± 0.2 L m⁻² h⁻¹. It is likely that a layer of organic

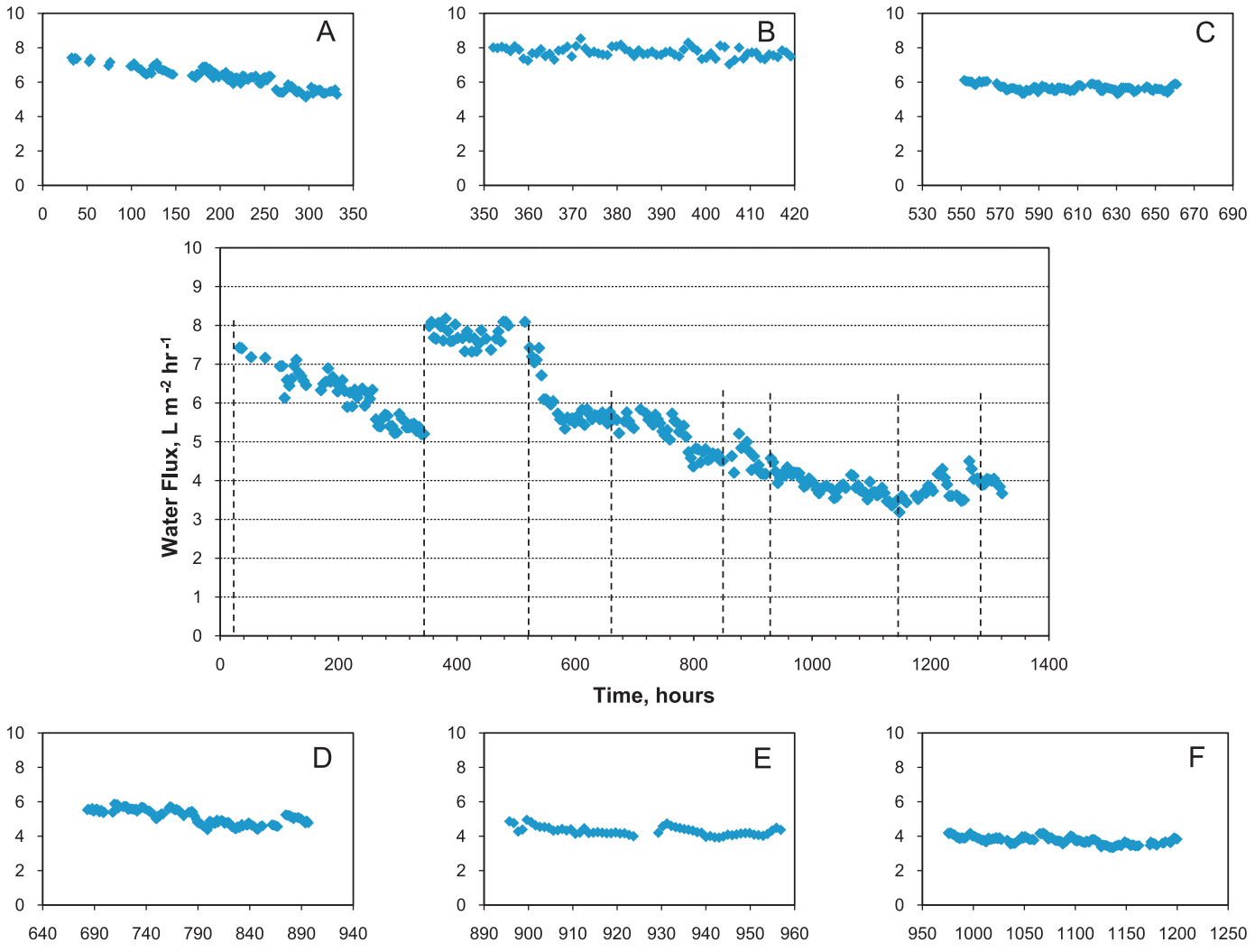


Fig. 2. Compiled water flux data from upgraded pilot-scale system. Letters marked on graph indicate intervals of interest during the pilot study and are defined in Table 4. Sub-plots provide enhanced views of water flux during each operation interval and have the same axis values as the central plot.

foulants accumulated on the membrane surface and reached a terminal thickness. The fouling layer can affect rejection of feed constituents [38,39] but will also increase resistance to water transfer through the membrane [39,40].

Once steady-state water flux was observed, the DS concentration was doubled at the beginning of interval B. Although the driving force for the FO process (i.e., the osmotic pressure of the DS) was doubled during interval B, water flux did not increase proportionally. This phenomenon is attributed to internal concentration polarization (ICP) phenomenon [41–43]. During 100 h of operation in interval B, water flux exhibited a marginal decrease from an average of 7.8 to an average of 7.5 L m⁻² h⁻¹. The small flux decline observed during this period indicates that after the initial fouling layer accumulated on the FO membrane (interval A), the membrane achieves remarkably consistent water productivity even when increasing its throughput. The system also achieved this stable performance despite a noticeable build up of mineral precipitates within the RO subsystem (observed in the DS rotameter of the RO subsystem).

Sample analysis indicated that two sparingly soluble salts, SrSO $_4$ and CaSO $_4 \cdot 2H_2O$, were most likely the cause of mineral scaling within the RO subsystem. Calculation of the initial percent saturation (OLI Analyzer v3.0, OLI Systems Incorporated, Morris Plains, NJ) of SrSO $_4$ was 52% and CaSO $_4 \cdot 2H_2O$ was 38% in a fresh 55,000 mg L $^{-1}$ sea salt. DS constituent concentrations measured in

the first sample taken from the RO subsystem revealed that these two mineral salts were supersaturated; yet, mineral scaling did not reduce water productivity of the hybrid process. A gradual increase in pressure drop (4.1 to 5.5 psig) through the DS channel of the FO membrane element indicated that precipitation of salts occurred on the DS spacer; however, the FO support layer surface is protected from mineral scaling by the continuous dilution of DS at the bulk DS—membrane interface with water diffusing through the membrane from the feed into the DS. Chemical cleaning of the RO subsystem was performed between interval B and C to remove mineral scale. The operating pressure required by the RO subsystem to maintain the DS concentration was reduced by approximately 13% after the cleaning.

During interval C, DS concentration was reduced to approximately 30,000 mg L^{-1} sea salt. Results indicate that the hybrid process rapidly achieved the same steady-state water flux performance observed at the end of interval A (5.7 \pm 0.2 L m $^{-2}~h^{-1}$), despite a substantial increase in water flux through the FO membrane during interval B. No change in pressure drop between either feed or DS inlets and outlets was detected throughout interval C (data not shown), indicating that foulants and debris were not accumulating in the membrane feed channels, and scaling was not occurring in the DS channels.

During the first $100\,h$ of interval D the FO feed stream contained approximately $5\,mg\,L^{-1}$ TSS, and after $100\,h$ it was

increased to approximately 16 mg L⁻¹ TSS. In both cases the feed TSS concentration was measured before the FO membrane element, after screening with a 50-mesh strainer. Minimal flux decline was observed during treatment of 5 mg L⁻¹ TSS feed; however, flux decreased from 5.3 to 4.6 L m⁻² h⁻¹ after feed TSS concentration increased to 16 mg L⁻¹. Pressure drop across the feed channel of the FO element did not increase during treatment of 5 mg L⁻¹ TSS feed, thus the membrane element appears to be suitable for treatment of municipal treated wastewater effluents with TSS concentrations of 5 mg L⁻¹ or lower. During treatment of 16 mg L⁻¹ TSS the pressure drop across the feed channels increased at a rate of 0.25 psig per day and stabilized after 115 h of operation following the increase in TSS concentration. Thus, steady-state operation of the system treating a feed with three times higher TSS concentration and with only 24% decrease in water flux expands the operating envelop of the hybrid process for many types of secondary effluent [44]. It is likely that operation with higher feed flow rate would have reduced feed channel blockage and improve process performance [13,18,45,46].

Immediately following interval D, the direction of feed flow within the FO membrane element was reversed for one hour in an attempt to remove settled suspended solids from the feed channels of the membrane element. Subsequently, normal operation conditions were resumed (feed flowing downward) and the initial water flux improved by approximately 15% to $5.3 \, \mathrm{L} \, \mathrm{m}^{-2} \, h^{-1}$. The hybrid process operated for 24 h before water flux returned to the value observed prior to flow reversal. Operating the system with a daily (likely automated) feed flow reversal may substantially increase water productivity of the FO membrane and may reduce the total number of FO elements required for sustained treatment of secondary treated wastewater effluents or similar streams.

The dosing rate of activated sludge was increased to a maximum of 50 mg L⁻¹ TSS after interval D. The dosing scheme consisted of 50 mg L⁻¹ TSS for 18 h followed by 6 h of 15 mg L⁻¹ TSS. This was necessary to reduce sludge buildup and eventual plugging of the 50-mesh feed screen during overnight operation. Despite the variability of TSS concentration in the feed, water flux exhibited only minor variation throughout this interval. Membrane fouling did occur and water flux declined by 0.7 L m⁻² h⁻¹ over a 34 h period; however, water flux rebounded after the 34 h of operation. Sloughing of activated sludge from the membrane surface and flushing out of the FO membrane element may have caused the sudden increase in water flux after 34 h from the beginning of interval E. Following this event, water flux declined more rapidly but reached a steady-state value after 9 h. A second water flux increase was observed after 60 h of operation in interval E, which may also correspond to an activated sludge deposit sloughing off the membrane. This hypothesis is further supported by a corresponding pressure drop decrease across the FO membrane element feed channel of 20% during both water flux increase events. As the activated sludge layer sloughs off the membrane it may open flow channels for the feed solution and therefore decrease the hydraulic resistance of flow through the membrane element.

During interval F the hybrid process operated with minimal interruption for 225 h while treating SBMBR permeate dosed with activated sludge to achieve approximately 16 mg $\rm L^{-1}$ TSS in the FO feed stream. Water flux decreased by less than 5% during this interval from 4.1 to $3.9\,\rm L\,m^{-2}~h^{-1}$. Despite considerable TSS loading during interval E and continued loading of TSS throughout interval F the system was able to maintain water productivity for a sustained period of time with minimal operator oversight and no chemical or physical cleaning of any kind.

Lastly, FO feed pressure was increased during interval G to simulate operation of a lead element in a multi-element pressure vessel. Feed inlet pressure was increased sequentially from 10 to

20 psig after 20 and 60 h of operation, respectively. Backpressure on the FO element feed line was relieved after 112 h of operation. Higher hydraulic pressure increased the permeation of water across the FO membrane and may have also increased the rate that foulants deposit on the membrane surface [30]. Water flux initially increased and then quickly decreased when 10 psig of hydraulic pressure was applied to the feed side of the membrane. In addition to an increased loading of membrane foulants from convective transport, increased hydraulic pressure may also compact the activated sludge layer on the membrane surface. The compacted sludge layer will increase mass transfer resistance through the membrane [40] and therefore decrease water flux. Water flux initially increased when 20 psig of hydraulic pressure was applied to the feed side of the membrane. Decline in water flux was observed for the first 10 h of operation with the higher applied feed pressure. Following the initial decline in water productivity, water flux was stable for the next 40 h of operation. The water flux decreased when the backpressure was removed from the FO element, and the element returned to the same water flux measured at the beginning of interval G. This result may indicate that the foulant layer was not irreversibly compacted and the fouling layer was able to rebound to the less-compact structure typically associated with organic fouling on FO membranes [18].

3.1.2. Fouling recovery

Previously we described flux recovery between interval D and E by performing a brief reversal of the direction feed flow through the element. A more thorough investigation of membrane fouling reversibility was also conducted. A second spiral wound element from the same membrane cast treated feed water with characteristics identical to those defined in interval C (Table 4). A plot of water flux achieved by the hybrid process as a function of time during the membrane fouling recovery study is shown in Fig. 3. Similar to the performance of the first FO spiral wound membrane, water flux was observed to decrease sharply in the early stage of the experiment before stabilizing at approximately 4.5 L m⁻² h⁻¹ after 50 h. Stable water flux was likely achieved more rapidly in this case compared to the previous experiment (Fig. 2) because the FO membrane was immediately exposed to a feed stream (SBMBR effluent) dosed with activated sludge. Water flux continued to decrease at a slower rate until approximately 240 h of operation when a sequence of physical and chemical cleaning cycles were performed on the FO membrane. After cleaning, water flux immediately improved by approximately 46% to $4.8 \pm 0.1 \,\mathrm{L\,m^{-2}\,h^{-1}}$. A second cleaning event was performed after additional 115 h (hour 355), but this time only marginal recovery of

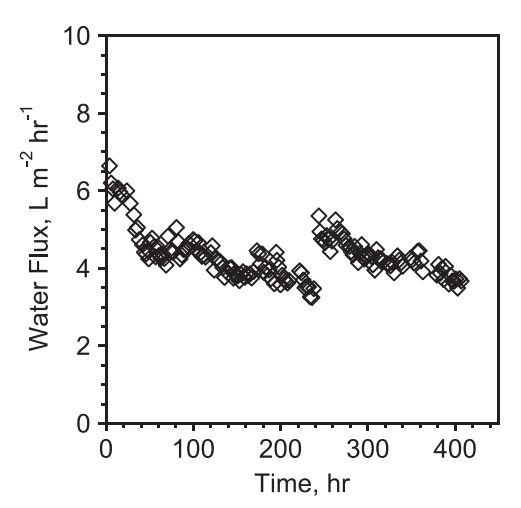


Fig. 3. Water flux as a function of time for membrane cleaning study.

flux was observed. It is likely that more channels in the corrugated feed spacer became plugged with solids and were not able to be cleaned under the tested conditions.

3.2. Solute transport through the membrane

3.2.1. Diffusion of DS solutes through RO and FO membranes

Typical first stage RO membrane recovery in the system was 4–6% and water flux was 3.9–8.1 L m $^{-2}$ h $^{-1}$, depending on operating conditions. The membrane manufacturer reports 99.4% rejection of NaCl at 8% element recovery and 38.7 L m $^{-2}$ h $^{-1}$ [28]; however, when operating at lower water recovery, less water permeates through the membrane to dilute co-diffusing solutes, and thus salt rejection is lower. During this study, first stage RO permeate rejection of NaCl was between 95 and 97%. Greater loss of DS solutes is expected from their reverse diffusion through the FO membrane.

DS solute fluxes through the FO membrane (reverse flux) and through the first stage RO membrane during intervals B. C. and D are summarized in Table 5. Both monovalent and divalent ions are able to permeate through the FO membrane faster than through the RO membrane as implied from membrane characteristics reported in Table 1. Yet an additional observation from this data set is that the reduced solvent/solute selectivity does not result in a uniform increase in monovalent and divalent ion permeation. Instead, divalent ions are observed to permeate through the FO membrane at an even greater relative rate than monovalent ions when compared to their same relative rates of permeation through the RO membrane. Additionally, with only the first stage membrane permeate being removed from the system, the lower concentration gradient of solutes on the first element generally also reduces solute loss compared to the FO element. Specific reverse flux of DS solutes during interval B was $2063 \pm 196 \text{ mg L}^{-1}$ TDS, and electroneutrality of diffusing solutes was maintained within acceptable measurement error [47] for solutes diffusing through the FO membrane and RO membrane (3.8 meg/L and -1.8 meq/L, respectively). And lastly, it is possible that cakeenhanced concentration polarization [48] on the FO membrane feed side during interval D was the reason for lower reverse solute flux through the FO membrane (Table 5).

The specific reverse solute flux measured during this study through the FO membrane (approximately 2200 mg L⁻¹) was substantially greater than that measured in previous bench-scale experiments (approximately 475 mg L⁻¹) with a synthetic sea salt DS and secondary treated wastewater effluent feed [10]; however, similar results were reported in another bench-scale study that used similar membrane, a 1.5 M NaCl DS, and activated sludge from an MBR as feed [49]. One possible explanation for the high specific reverse diffusion observed in our pilot study is that uneven flow in the DS channels inside the FO membrane envelop created localized dead-zones where poor mixing of the DS

reduced local water flux and increased reverse diffusion of DS solutes. Another possibility for the high specific reverse diffusion observed in our study is that the membrane employed consists of a much larger surface area compared to bench-scale studies and is comprised of material from a single, continuous cast. Being a prototype membrane, this may lend itself to more frequent material aberrations in the form of pinholes or other microdefects that are unable to selectively permeate water instead of solutes. By removing the barrier that inhibits permeation of these solutes they will tend to diffuse at their uninhibited natural rate. It is probable that the occurrence of membrane defects is less likely in the hand-selected membranes typically employed for benchscale testing. However, in this study the FO feed stream was maintained at a higher pressure than the DS to reduce strain on the glue seams of the membrane; thus, the net permeation of DS solutes would be less than their natural rate of diffusion due to convective drag forces imposed by the solvent (water).

Membrane fouling may also affect reverse solute permeation rate through the membrane, especially if reverse diffusing solutes become trapped in the fouling cake layer on the feed side of the membrane [48,50]. A higher concentration of DS solutes at the feed-membrane interface may reduce the driving force for reverse solute diffusion. While cake enhanced osmotic pressure on the feed solution side may have reduced water flux, it is also possible that the observed, relatively open structure of the fouling layer does not substantially inhibit reverse permeating draw solutes from reaching the bulk feed solution. In this case, the lower retention of draw solutes by the membrane may itself be the cause of reduced water flux. Reverse solute flux was calculated from measured solute concentration in samples drawn after 120 h of operation during interval D. Prior to the exposure of the membrane to mixed liquor solids, all solutes, except strontium, had substantially greater reverse solute flux. Reverse solute flux for five of the eight solutes during interval D was reduced by similar percentages (16.8 \pm 4.0%) compared to equivalent values in interval C. Water flux decreased by a similar percentage (13.4%) during the same time interval. A specific reverse solute flux of $2211 \pm 205 \text{ mg L}^{-1}$ was calculated for data shown in Table 5 for interval D. The higher permeation rate of divalent ions through the FO membrane compared to the RO membrane may be explained in terms of traditional solute/solvent selectivity and solutiondiffusion permeation models [51,52].

3.2.2. Rejection of nutrients by the hybrid FO-RO process

Orthophosphate and nitrate concentrations in the feed are summarized in Table 3. Rejection of these constituents by the FO and RO membranes individually and the total rejection by the hybrid FO–RO process during intervals B through E are shown in Fig. 4a for orthophosphate and Fig. 4b for nitrate. Average orthophosphate rejection for data presented in Fig. 4a was 99.6, 99.6, and > 99.99% for the FO membrane, RO membrane, and total

Table 5DS reverse solute flux through the FO membrane and DS solute leakage through the first stage RO membrane during intervals B, C, and D.

Constituent	Interval B solute flux $\mathrm{mg}~\mathrm{m}^{-2}~\mathrm{h}^{-1}$		Interval C solute flux $mg m^{-2} h^{-1}$		Interval D solute flux $\mathrm{mg}~\mathrm{m}^{-2}~\mathrm{h}^{-1}$	
	FO	RO	FO	RO	FO	RO
Boron	6.5 ± 1.4	N.D.	_	_	_	_
Calcium	425 ± 51	16.7 ± 0.1	160 ± 5.0	8.2 ± 2.4	160 ± 9.0	12.0 ± 1.0
Magnesium	875 ± 70	62.0 ± 11.0	430 ± 50	21.3 ± 6.4	370 ± 50	34.0 ± 3.0
Potassium	269 ± 68	54.0 ± 1.0	180 ± 6.0	30.0 ± 5.6	157 ± 4.0	33.0 ± 5.0
Sodium	4162 ± 395	1700 ± 50	4110 ± 210	860 ± 160	3550 ± 310	940 ± 170
Strontium	10.5 ± 2.9	0.4 ± 0.1	2.9 ± 1.3	0.1 ± 0.0	3.0 ± 0.4	0.2 ± 0.0
Bromide	53.4 ± 10.6	9.7 ± 0.2	106 ± 91	5.8 ± 0.7	39.0 ± 3.0	6.0 ± 1.0
Chloride	8480 ± 810	2830 ± 120	7410 ± 440	1414 ± 250	6210 ± 80	1540 ± 280
Sulfate	1890 ± 180	160 ± 30	990 ± 150	50 ± 14	750 ± 70	79.0 ± 8.0

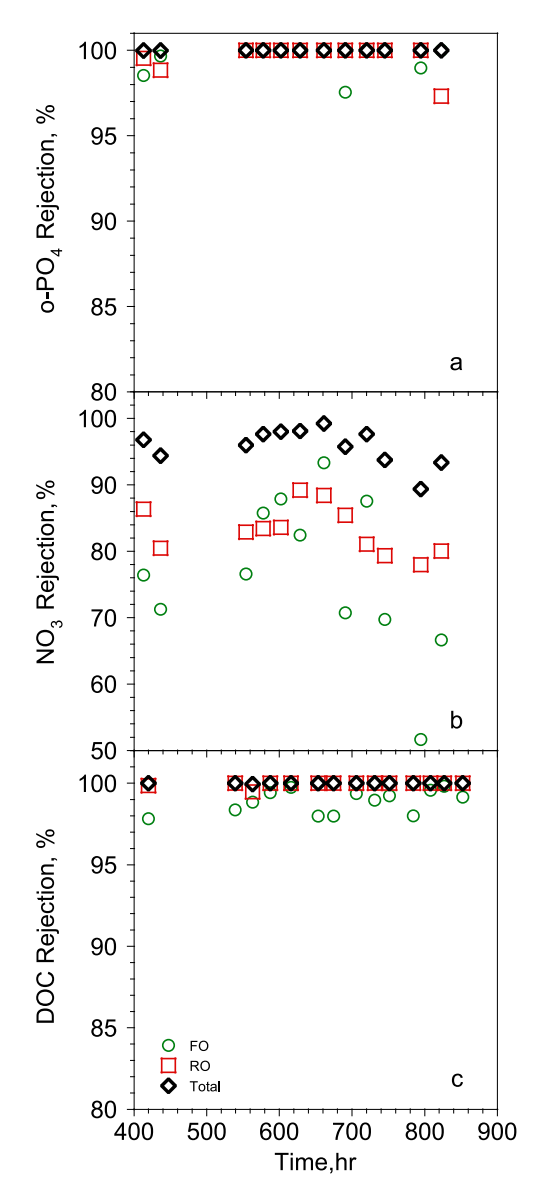


Fig. 4. Rejection of (a) ortho-phosphate, (b) nitrate, and (c) DOC by the FO and RO membranes and total rejection by the hybrid FO–RO process beginning 100 hours into interval B and lasting into interval E.

hybrid process rejection, respectively. High rejection of orthophosphate affirms previous observations [53,54].

Average nitrate rejection for data presented in Fig. 4b was 76.7, 83.2, and 95.8% for the FO membrane, RO membrane, and total hybrid process rejection, respectively. Moderate nitrate rejection of both the FO and RO membrane is expected based on previous studies [10,17,30,55–58]; however, the relatively high total rejection of nitrate by the hybrid process produces product water quality between five to ten times lower than the United States Environmental Protection Agency Maximum Contaminant Level (MCL) for nitrate in drinking water (10 mg-N L⁻¹) [59].

3.2.3. Transport of organic matter

TSS concentrations of the feed, DS, and product water indicate that TSS was completely rejected by the FO membrane and no additional removal was achieved with the RO membrane. This result is expected because both the FO and RO membranes are dense, non-porous barriers [26,30].

DOC concentration in the feed stream is reported in Table 3 and DOC rejection by the hybrid process and the individual membrane

processes during intervals B through E is shown in Fig. 4c. Average rejection of DOC by the FO and RO membranes was high (98.6 \pm 2.0 and 99.8 \pm 0.4%, respectively) for intervals B through E, and the total rejection of DOC by the hybrid process was greater than 99.9% for all samples analyzed. DOC concentration in the RO product water was at or below the detection limit for the TOC analyzer. These results demonstrate the robustness and reliability of the hybrid FO–RO process to protect product water from DOC present in impaired feed streams.

Mass flux of DOC through the FO membrane varied depending on system operating conditions. The highest mass flux of DOC through the FO membrane was observed during interval B $(0.65 + 0.10 \text{ mg m}^{-2} \text{ h}^{-1})$. Enhanced external concentrative concentration polarization of constituents at the membrane-feed interface resulting from increased water flux (relative to intervals C through E) may account for the elevated DOC flux observed during interval B. Average DOC flux through the FO membrane during interval C decreased by 53% compared to interval B $(0.30 + 0.11 \text{ mg m}^{-2} \text{ h}^{-1})$. Reduced water flux through the FO membrane may account for the reduction in DOC flux through the membrane as less DOC is accumulated at the membrane surface. DOC flux was reduced by an additional 15% during intervals D and E relative to interval C (0.26 \pm 0.12 mg m⁻² h⁻¹). Activated sludge from the SBMBR likely produced an organic cake layer on the membrane surface that enhanced rejection of DOC. This concept is supported by a previous study [60], which observed that accumulation of organic matter on the surface of nanofiltration membranes will enhance the rejection of DOC. Complexation of calcium with the DOC at the membrane-feed interface may also bind DOC, and in the absence of hydraulic pressure it will form loose layers of a conglomerated organic mass that does not strongly associate with the membrane [19]. If the DOC is not compacted against the active layer, but instead held in suspension above it, then its ability to partition and permeate through the membrane may be reduced.

SUVA measurements of feed and DS samples provided additional insight into DOC removal by the FO membrane. Waters with a high humic acid fraction have SUVAs between 3 and $5\,\mathrm{L\,mg^{-1}\,m^{-1}}$, while waters with a low humic acid fraction are generally less than $2\,\mathrm{L\,mg^{-1}\,m^{-1}}$ [30]. SUVA of the FO feed water was $2.37\pm0.11\,\mathrm{L\,mg^{-1}\,m^{-1}}$ for samples drawn from the system between interval B and D. SUVA of DS samples drawn simultaneously from the system were on average $0.25\pm0.12\,\mathrm{L\,mg^{-1}\,m^{-1}}$ lower than corresponding feed samples. This may indicate that proportionally less of the humic acid fraction of DOC present in the feed diffuses through the FO membrane. Enhanced rejection of humic acids over other DOC fractions (i.e., fulvic acid or low molecular weight acids) is expected because the molecular weight of humic acid ranges up to 200,000 g mol⁻¹ compared to fulvic acid that varies between 200 and 1000 g mol⁻¹ [47].

A recent study by Yangali-Quintanilla et al. [11] evaluated similar factors to our previous study [10] and confirmed several claims related to membrane fouling resistance at the bench scale and efficacy of the dual barrier process for contaminant removal. Yangali-Quintanilla et al. used a liquid chromatography organic carbon analyzer to verify that a batch-operated bench-scale FO membrane cell achieves high apparent rejection of biopolymers, humic substances, building blocks, and low molecular weight acids; however, accumulation of DOC (most likely from low molecular weight neutrally charged organic compounds) in the DS was still observed.

In the current study we also evaluate the characteristics of feed water DOC that was able to diffuse through the FO membrane by measuring fluorescence and reporting EEMs of FO feed, DS, and RO permeate. A sequence of feed and DS EEMs normalized by sample DOC concentration and representative of specific operation

intervals with and without dosing of activated sludge (i.e., interval B through C and interval D through E, respectively) is shown in Fig. 5. Dosing activated sludge from the SBMBR during intervals D and E enhanced peak T_1 signature (left bottom corner) in feed EEMs (left column in Fig. 5). Feed EEMs from intervals D and E indicate that adding activated sludge into the SBMBR permeate increased the mass loading of protein-like DOC onto the FO membrane. DS EEMs (middle column in Fig. 5) indicate that fluorophore response peaks previously identified in feed EEMs are still present. This suggests that a fraction of the DOC that was able to diffuse through the FO membrane is similar to DOC in the feed: however, the differential EEMs (right column in Fig. 5 produced by subtracting a corresponding DS EEM from feed EEM) indicate that a broad class of fluorophores is partially removed by the FO membrane. During intervals B and C these fluorophores are predominantly associated with humic acid- and fulvic acid-like constituents. Enhanced removal of protein-like fluorophores (peak T_1) during intervals D and E compared to intervals B and C is observed. High molecular weight proteins introduced during dosing of activated sludge into the feed were likely well rejected by the FO membrane, while low molecular weight protein-like fluorophores (e.g., tryptophan or other types of amino acids with phenyl groups) were poorly rejected by the FO membrane.

FO feed, DS, and RO permeate EEMs collected over a continuous week of operation during interval C are illustrated in Fig. 6. Unlike in Fig. 5, EEMs shown in Fig. 6 are not normalized by sample DOC concentration. The signature of DOC in feed sample EEMs (left column) were relatively consistent during this period. The DS hydraulic system was drained, rinsed, and refilled with fresh DS at the beginning of interval C (day 1). DS EEM at day 1 indicates that the commercial synthetic sea salt does not contain a significant concentration of fluorophores in correlation with its relatively low DOC concentration (0.9 mg $\rm L^{-1}$). Accumulation of fluorophores in the DS can be observed in the middle column of EEMs. During the one-week interval a gradual increase in the intensity of all three fluorescence peaks is observed. The intensities of peaks A and T_1

(representative of fulvic- and protein-like DOC, respectively) appear to increase at a slightly faster rate than peak *C* (humic-like DOC) in agreement with a size exclusion DOC rejection mechanism and assuming that the protein-like peak is mostly composed of low molecular weight amino acids. RO permeate EEMs are presented with half the intensity scale of corresponding feed and DS EEMs. There are no discernable fluorescence signatures in permeate samples, and DOC concentration in the product water was below detection limit for the analytical method employed.

3.3. Membrane autopsy

Membrane autopsy was performed after 1300 consecutive hours (55 days) of operation. Visual inspection revealed few continuous activated sludge deposits on the active layer of the FO membrane. Visual inspection of RO membranes observed small, dispersed inorganic crystals on membrane surfaces.

3.3.1. FO membrane fouling and its effect on membrane surface properties

FO membrane samples extracted from the membrane leaf were gently rinsed with deionized water prior to analysis. SEM micrographs of the support side of the FO membrane did not show any bacteria or organic matter (micrograph not shown). Mineral deposits were also not detected on the support surface, which provides further evidence that the dilution effect of DS at the support layer-DS interface mitigates mineral scale formation at this interface.

Substantial portion of the activated sludge deposited on the FO membrane was removed during the rinsing process, indicating that the fouling layer was not strongly adhered to the membrane surface. A sequence of FESEM micrographs of the boundary region between an activated sludge cake layer on the FO membrane and the exposed active layer of the FO membrane is shown in Fig. 7. The last micrograph in the sequence shows that only small

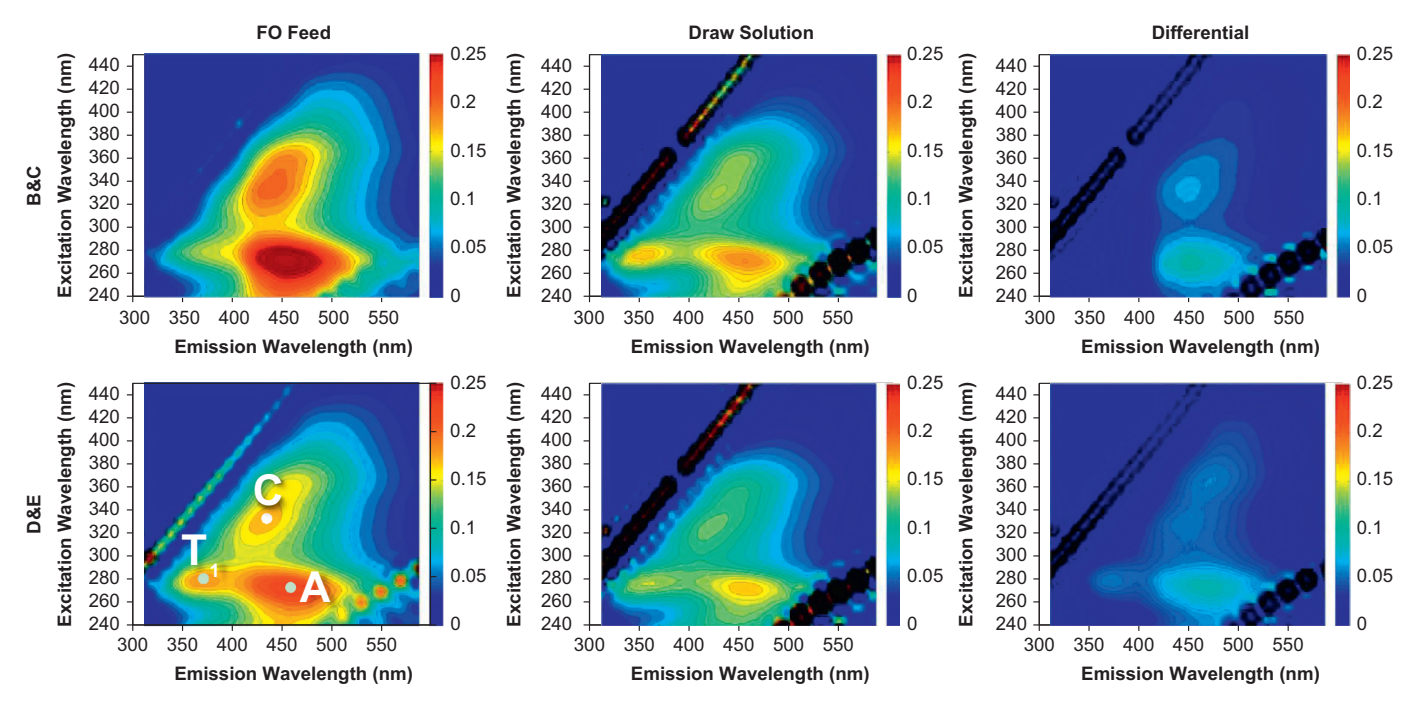


Fig. 5. Comparison of feed (left column), DS (middle column), and differential (right column) EEMs from representative samples taken during intervals B through E of this study. All EEMs intensities are in Raman units normalized by sample DOC concentration. The A, B, and T1 peaks common to EEMs are enumerated on the bottom left figure.

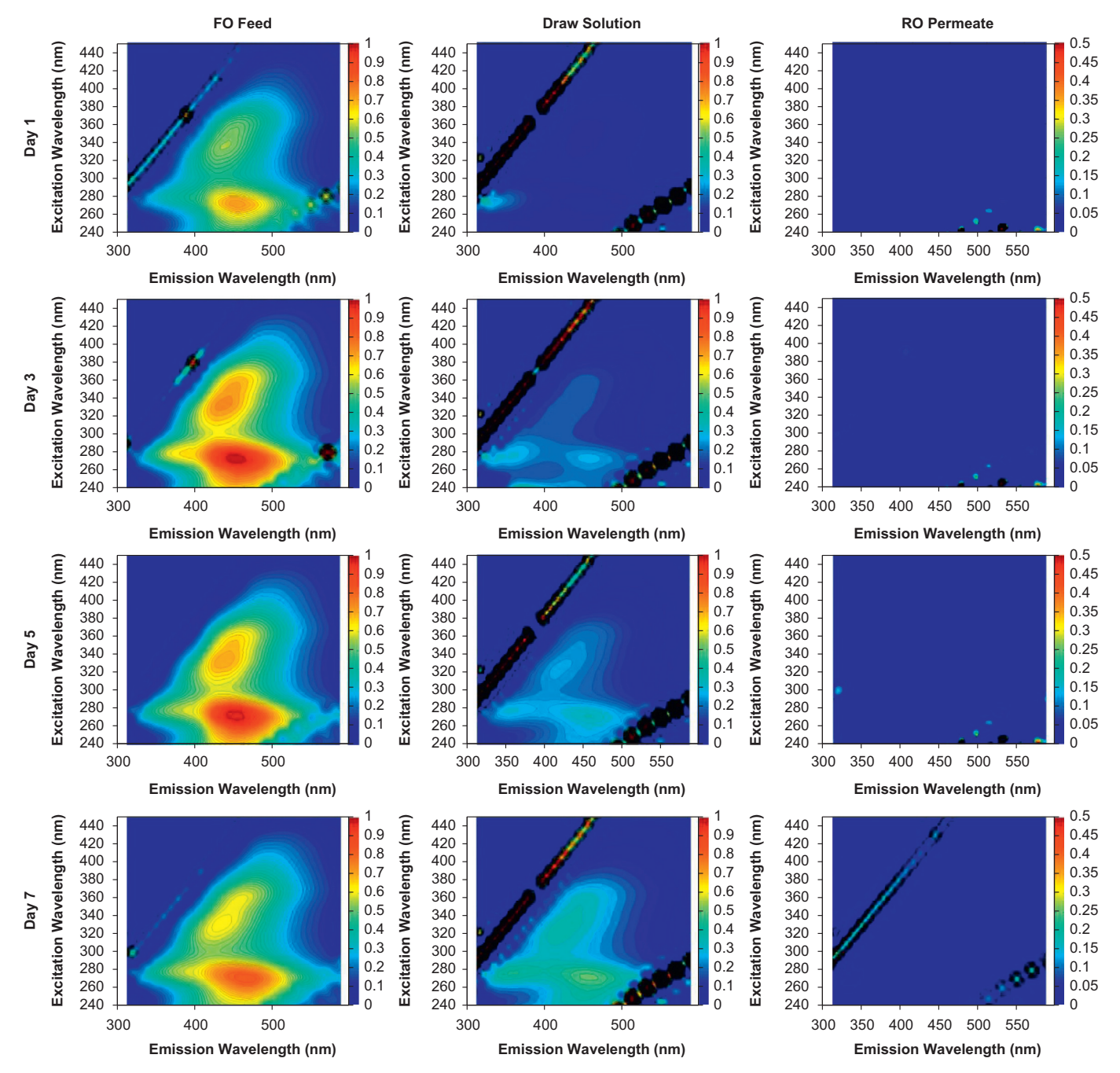


Fig. 6. Comparison of feed (left column), DS (middle column), and RO product water (right column) EEMs during intervals B through E of this study. All EEMs intensities are in Raman units, feed and DS samples are normalized by DOC concentration. Product water EEMs intensity is half the range of DS and feed samples.

particles remain on the membrane surface after mild washing, indicating that the sludge layer is loosely bound to the membrane surface. FTIR-ATR spectra also confirmed that the fouling layer on the active surface of the FO membrane does not produce measurable infrared absorbance and is therefore exceedingly thin (data not shown)

Fluorescence microscopy was also employed to investigate biofouling on the membrane. The fluorescence micrograph of the membrane active layer (Fig. 8a) indicates deposition of soluble microbial products and extracellular biological organic matter on the surface of the membrane. Linear features observed on the support layer of the membrane (Fig. 8b) are the woven support mesh. Faint circular features are likely pores that extend to the active layer of the membrane. There were no signatures of bacteria or microbial byproducts on the support side of the membrane.

Although the fouling layer on the active side of the membrane was easily removed by rinsing, surface properties of FO membranes were changed as a result of fouling. The FO membrane is observed to become more hydrophilic when fouled by activated sludge from the SBMBR system, with contact angle decreasing from $73.7\pm2.0^\circ$ for virgin membrane to between $64.3\pm1.7^\circ$ (inlet center) and $60.7\pm4.8^\circ$ (inlet outer edge) of used membranes. The hydrophobicity differences between the different membranes samples was found to be statistically insignificant. This indicates that the organic foulants affected the surface hydrophobicity similarly despite likely variations in the local DS concentration and flow distribution.

Zeta potential measurements were conducted to quantify the surface charge of the membranes and investigate the result of fouling on membrane surface charge (Fig. 9). FO membranes exposed to domestic wastewater effluent became more negatively

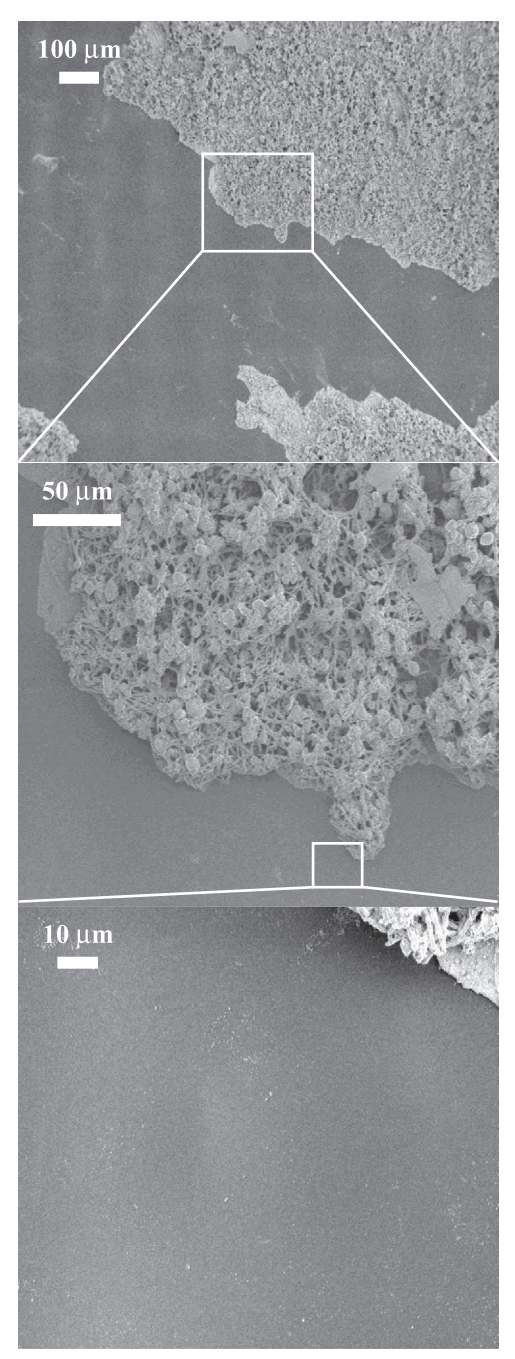


Fig. 7. FESEM micrographs of FO membrane active layer.

charged than the virgin FO membrane. These results corroborate findings from contact angle measurements of the FO membrane. Recent research on the effect of membrane surface charge and solute permeation behavior indicates that the increasing negative charge could affect the type of coupled solute diffusion observed [61]. Namely, increasing negative surface charge appears to favor sodium ion permeation and may partially account for relatively high reverse salt flux observed during operation.

3.3.2. Evaluation of FO membrane integrity

NaCl salt rejection was measured for two FO membrane samples extracted from both inlet locations (near the central collection/ distribution tube and at the outer edge of the membrane leaf), and for new FO membrane. NaCl rejections by the virgin membrane,

fouled membrane removed from near the core tube at the feed inlet, and fouled membrane removed from the outer edge of the leaf were 93.2 \pm 0.9%, 92.3 \pm 0.2%, and 91.4 \pm 1.0%, respectively. A statistically insignificant difference was found between NaCl rejection values for all membrane samples.

The rejection of NaCl for all FO membrane samples is similar to values reported for tight NF membranes (e.g., greater than 90 percent sodium rejection and molecular weight cut-off (MWCO) less than 200 Da [62]); yet, sample fluorescence measurements indicate that DOC with molecular weights exceeding 200 Da (e.g., fulvic and humic acids) was able to accumulate in the DS. FESEM was employed to examine the active layer of the FO membrane samples for any surface defects that may help to explain the transport of higher molecular weight DOC fractions and the relatively high reverse solute flux reported previously. An FESEM micrograph of the FO membrane active layer is shown in Fig. 10. White circles indicate possible membrane defects that may provide a path for larger molecular weight compounds to transport through the membrane. Both features are approximately 100 nm in width and may provide a conduit for DOC with characteristic lengths less than 100 nm (e.g., fulvic and amino acids) to permeate through the membrane. White deposits on the membrane surface are associated with bacteria and colloids from the feed.

3.3.3. Autopsy of RO membranes

Review of scanning electron micrographs did not reveal appreciable differences between the feed inlet and the concentrate outlet for any of the RO elements. Small, dispersed mineral crystals were infrequently observed on the membrane surface (micrographs not shown) and EDS analysis was performed on the individual particles observed on the RO membranes. Particles detected on the surface of the first stage RO membrane were primarily composed of calcium and sulfate, which were likely formed by minerals from the DS. Interestingly, different deposits with calcium, sulfate, and silica signatures were observed in the third stage element. It is possible that silica colloids were catalyzed by the increasing concentration of calcium ions in the final RO element [63]. These results provide visual indications that the RO membranes were minimally affected by organic foulants from the SBMBR feed stream and only negligible precipitation of DS salts occurred. Furthermore, the RO membranes fully recovered from the mineral scale event observed during operation interval B.

Contact angle measurement using the sessile drop method indicated that the RO membrane became more hydrophobic with contact angle increasing from $38\pm1.9^\circ$ to $57\pm3.4^\circ$ (feed end) and $66\pm4.7^\circ$ (concentrate end). There is no difference in hydrophobicity between the first and third RO element, but the feed end is consistently more hydrophobic than the concentrate end. This may be caused by the diffusion and adsorption of hydrophobic organic matter from the FO permeate onto the RO membrane, or it may also be understood from the prospective of the development of a inorganic scaling layer on the membrane. The adsorption of negatively charged matter on RO membranes is confirmed by the streaming potential measurement (Fig. 11). After 55 days of operation, the SW30 membranes became more negatively charged, and the degree of surface charge is similar between the first stage and third stage.

4. Conclusions

In the current study a hybrid, dual barrier, FO–RO process was investigated at the pilot scale. The FO membrane employed in this study was capable of maintaining acceptable water flux despite high loading of dissolved and suspended materials typically avoided in RO applications. The concentrations of all constituents found in the feed water were reduced by the dual barrier process

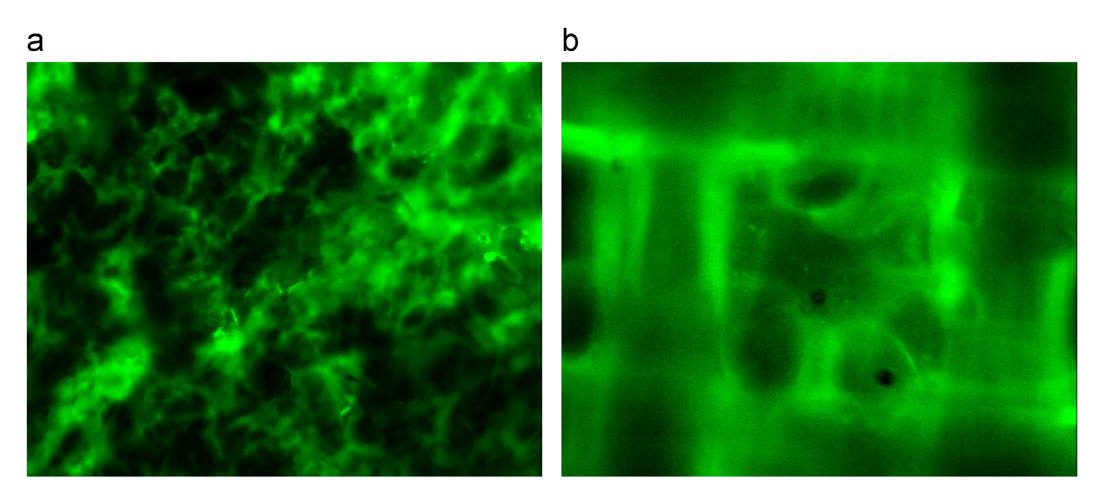


Fig. 8. Fluorescence micrographs of the (a) the active layer and (b) the support layer of the FO membrane stained with SYBR green dye.

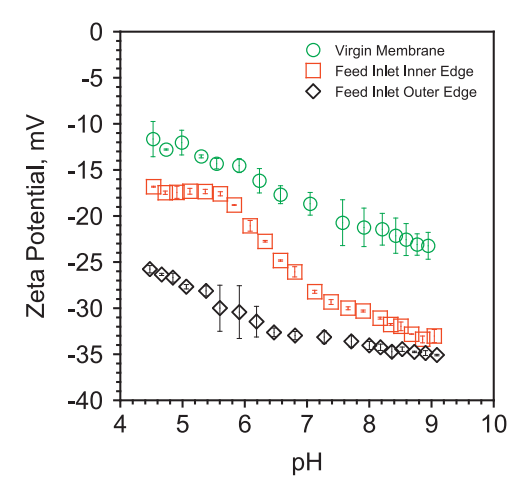


Fig. 9. Streaming potential measurements of FO membrane samples.

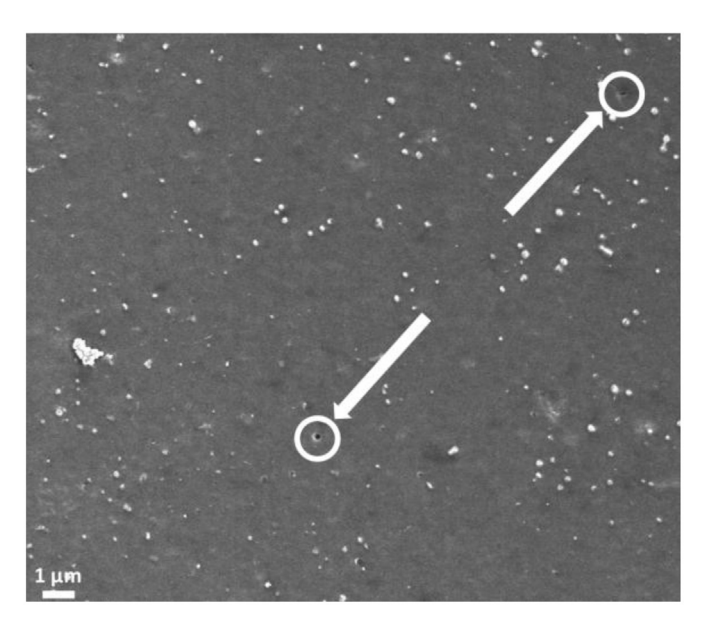


Fig. 10. An FESEM micrograph of FO membrane active layer showing possible defects in the active layer.

to levels lower than the EPA primary drinking water standards—making the RO permeate water drinkable and the process capable of treating impaired water for direct potable reuse. Unlike operation in a closed DS loop in which feed constituents will slowly

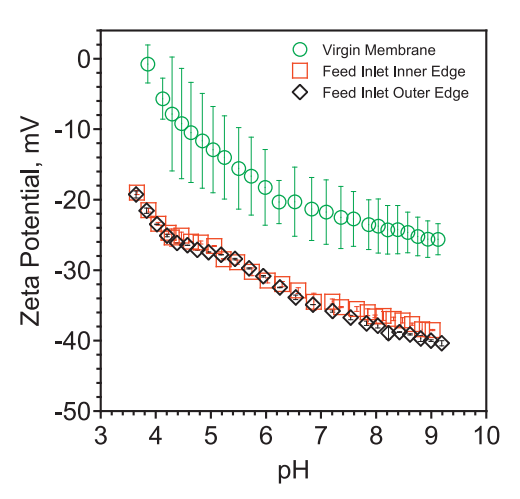


Fig. 11. Streaming potential of SW30 membrane samples.

accumulate in DS, when operated in osmotic dilution mode [10,11,16,64] the product water (RO permeate) will be even more purified due to lower concentration of feed constituents in the DS.

Although membrane fouling occurred in the feed channels of the spiral wound FO element, fouling was mostly reversible. In this study feed TSS concentration was exceptionally high and not representative of most feed streams. It is very likely that with higher FO feed flow rate and reasonable TSS concentration (<5 mg L $^{-1}$) spiral w\ound membranes with corrugated feed spacers will be suitable for sustainable treatment of effluents from most wastewater treatment plants.

Acknowledgments

The authors would like to acknowledge the agencies that contributed funding for this study. These include California Department of Water Resources (Grant 46-7446-R-08), Texas Water Development Board (TWDB Contract no. 0804830852), Research Partnership to Secure Energy for America (Grant 07122-12), and the AWWA Abel Wolman Fellowship.

References

 M.A. Shannon, P.W. Bohn, M. Elimelech, J.G. Georgiadis, B.J. Marinas, A.M. Mayers, Science and technology for water purification in the coming decades, Nature 452 (2008).

- [2] T. Asano, F. Burton, H. Leverenz, R. Tsuchihashi, G. Tchobanoglous, Water Reuse: Issues, Technologies, and Applications, McGraw-Hill, New York, 2007.
- [3] J.O. Kessler, C.D. Moody, Drinking water from sea water by forward osmosis, Desalination 18 (1976) 297–306.
- [4] S. Zhao, L. Zou, C.Y. Tang, D. Mulcahy, Recent developments in forward osmosis: opportunities and challenges, J. Membr. Sci. 396 (2012) 1–21.
- [5] T.Y. Cath, S. Gormly, E.G. Beaudry, T.F. Michael, V.D. Adams, A.E. Childress, Membrane contactor processes for wastewater reclamation in space: Part I. Direct osmosis concentration as pretreatment for reverse osmosis, J. Membr. Sci. 257 (2005) 85–98.
- [6] R.L. McGinnis, M. Elimelech, Energy requirements of ammonia-carbon dioxide forward osmosis desalination, Desalination 207 (2007) 370–382.
- [7] D.L. Shaffer, N.Y. Yip, J. Gilron, M. Elimelech, Seawater desalination for agriculture by integrated forward and reverse osmosis: improved product water quality for potentially less energy, J. Membr. Sci. 415–416 (2012) 1–8.
- [8] R.L. McGinnis, N.T. Hancock, M.S. Nowosielski-Slepowron, G.D. McGurgan, Pilot demonstration of the NH₃/CO₂ forward osmosis desalination process on high salinity brines, Desalination 312 (2013) 67–74.
- [9] R. Semiat, Energy issues in desalination processes, Environ. Sci. Technol. 42 (2008) 8193–8201.
- [10] T.Y. Cath, N.T. Hancock, C.D. Lundin, C. Hoppe-Jones, J.E. Drewes, A multi-barrier osmotic dilution process for simultaneous desalination and purification of impaired water, J. Membr. Sci. 362 (2010) 417–426.
- [11] V. Yangali-Quintanilla, Z. Li, R. Valladares, Q. Li, G. Amy, Indirect desalination of red sea water with forward osmosis and low pressure reverse osmosis for water reuse, Desalination 280 (2011) 160–166.
- [12] H. Zhu, L. Zhang, X. Wen, X. Huang, Feasibility of applying forward osmosis to the simultaneous thickening, digestion, and direct dewatering of waste activated sludge, Bioresour. Technol. 113 (2012) 207–213.
- [13] K.L. Hickenbottom, N.T. Hancock, N.R. Hutchings, E.W. Appleton, E.G. Beaudry, P. Xu, T.Y. Cath, Forward osmosis treatment of drilling mud and fracturing wastewater from oil and gas operations, Desalination 312 (2013) 60–66.
- [14] N.T. Hancock, N.D. Black, T.Y. Cath, A comparative life cycle assessment of hybrid osmotic dilution desalination and established seawater desalination and wastewater reclamation processes, Water Res. 46 (2012) 1145–1154.
- [15] T.Y. Cath, J.E. Drewes, C.D. Lundin, N.T. Hancock, Forward osmosis-reverse osmosis process offers a novel hybrid solution for water purification and reuse, Int. Desalination Assoc. 2 (2010) 16–20.
- [16] N.T. Hancock, P. Xu, D.M. Heil, C. Bellona, T.Y. Cath, Comprehensive bench- and pilot-scale investigation of trace organic compounds rejection by forward osmosis, Environ. Sci. Technol. 45 (2011) 8483–8490.
- [17] N.T. Hancock, T.Y. Cath, Solute coupled diffusion in osmotically driven membrane processes. Environ. Sci. Technol. 43 (2009) 6769–6775.
- [18] S. Lee, C. Boo, M. Elimelech, S. Hong, Comparison of fouling behavior in forward osmosis (fo) and reverse osmosis (ro), J. Membr. Sci. 365 (2010) 34–39.
- [19] B. Mi, M. Elimelech, Organic fouling of forward osmosis membranes: Fouling reversibility and cleaning without chemical reagents, J. Membr. Sci. 348 (2010) 337–345
- [20] X. Jin, J. Shan, C. Wang, J. Wei, C.Y. Tang, Rejection of pharmaceuticals by forward osmosis membranes, J. Hazard. Mater. 227–228 (2012) 55–61.
- [21] M. Xie, L.D. Nghiem, W.E. Price, M. Elimelech, Comparison of the removal of hydrophobic trace organic contaminants by forward osmosis and reverse osmosis, Water Res. 46 (2012) 2683–2692.
- [22] M. Xie, W.E. Price, L.D. Nghiem, Rejection of pharmaceutically active compounds by forward osmosis: role of solution ph and membrane orientation, Sep. Purif. Technol. 93 (2012) 107–114.
- [23] Sequencing batch membrane bioreactor, (http://aqwatec.mines.edu/research/ SBMBR/), 2012 (accessed on August 21).
- [24] Y.C. Kim, S.-J. Park, Experimental study of a 4040 spiral-wound forwardosmosis membrane module, Environ. Sci. Technol. 45 (2011) 7737–7745.
- [25] B. Gu, D.Y. Kim, J.H. Kim, D.R. Yang, Mathematical model of flat sheet membrane modules for fo process: plate-and-frame module and spiralwound module, J. Membr. Sci. 379 (2011) 403–415.
- [26] T.Y. Cath, A.E. Childress, M. Elimelech, Forward osmosis: principles, applications, and recent developments, J. Membr. Sci. 281 (2006) 70–87.
- [27] T.Y. Cath, M. Elimelech, J.R. McCutcheon, R.L. McGinnis, A. Achilli, D. Anastasio, A.R. Brady, A.E. Childress, I.V. Farr, N.T. Hancock, J. Lampi, L.D. Nghiem, M. Xie, N.Y. Yip, Standard methodology for evaluating membrane performance in osmotically driven membrane processes, Desalination 312 (2013) 31–38.
- [28] Water and process solutions, dow filmtec sw30-2540, (http://www.dowwater andprocess.com/products/membranes/sw30_2540.htm), 2012.
- [29] AWWA, Standard Methods for the Examination of Water and Wastewater, 21st, American Public Health Association, American Water Works Association, and Water and Environment Federation, Washington D.C., 2005.
- [30] R. Letterman, AWWA, Water quality and treatment: A Handbook of Community Water Supplies, 5th edition, McGraw-Hill, New York, 1999.
- [31] R.M. Cory, D.M. McKnight, Fluorescence spectroscopy reveals ubiquitous presence of oxidized and reduced quinones in dissolved organic matter, Environ. Sci. Technol. 39 (2005) 8142–8149.
- [32] T. Ohno, Fluorescence inner-filtering correction for determining the humification index of dissolved organic matter, Environ. Sci. Technol. 36 (2002) 742–746.
- [33] W. Chen, P. Westerhoff, J.A. Leenheer, K. Booksh, Fluorescence excitation ,åíemission matrix regional integration to quantify spectra for dissolved organic matter, Environ. Sci. Technol. 37 (2003) 5701–5710.

- [34] P.G. Coble, Characterization of marine and terrestrial dom in seawater using excitation–emission matrix spectroscopy, Mar. Chem. 51 (1996) 325 –246.
- [35] N. Hudson, A. Baker, D. Reynolds, Fluroescence analysis of dissolved organic matter in natural, waste and polluted waters—a review, River Res. Appl. 23 (2007) 631.
- [36] R.K. Henderson, A. Baker, K.R. Murphy, A. Hambly, R.M. Stuetz, S.J. Khan, Fluorescence as a potential monitoring tool for recycled water systems: a review, Water Res. 43 (2009) 863–881.
- [37] J. Drelich, J.D. Miller, R.J. Good, The effect of drop (bubble) size on advancing and receding contact angle for heterogeneous and rough solid surfaces as observed with sessile-drop and captive-bubble techniques, J. Colloid Interface Sci. 179 (1996) 37–50.
- [38] L.D. Nghiem, D. Vogel, S. Khan, Characterising humic acid fouling of nanofiltration membranes using bisphenol a as a molecular indicator, Water Res. 42 (2008) 4049–4058.
- [39] P. Xu, J.E. Drewes, T.-U. Kim, C. Bellona, G. Amy, Effect of membrane fouling on transport of organic contaminants in nf/ro membrane applications, J. Membr. Sci. 279 (2006) 165–175.
- [40] R.D. Cohen, R.F. Probstein, Colloidal fouling of reverse osmosis membranes, J. Colloid Interface Sci. 114 (1986) 194–207.
- [41] G.D. Mehta, S. Loeb, Internal polarization in the porous substructure of a semipermeable membrane under pressure-retarded osmosis, J. Membr. Sci. 4 (1978) 261.
- [42] S. Loeb, L. Titelman, E. Korngold, J. Freiman, Effect of porous support fabric on osmosis through a loeb-sourirajan type asymmetric membrane, J. Membr. Sci. 129 (1997) 243–249.
- [43] J.R. McCutcheon, M. Elimelech, Influence of concentrative and dilutive internal concentration polarization on flux behavior in forward osmosis, J. Membr. Sci. 284 (2006) 237–247.
- [44] G. Tchobanoglous, F.L. Burton, D. Stensel, Wastewater engineering, Treatment, Disposal and Reuse, 4th edition, McGraw-Hill, New York, 2003.
- [45] B. Mi, M. Elimelech, Chemical and physical aspects of organic fouling of forward osmosis membranes, J. Membr. Sci. 320 (2008) 292–302.
- [46] S. Zou, Y. Gu, D. Xiao, C.Y. Tang, The role of physical and chemical parameters on forward osmosis membrane fouling during algae separation, J. Membr. Sci. 366 (2011) 356–362.
- [47] J.C. Crittenden, R.R. Trussell, D.W. Hand, K.J. Howe, G. Tchobanoglous, Water Treatment: Principles and Design, 2nd edition, John Wiley & Sons, Inc., 2005.
- [48] C. Boo, S. Lee, M. Elimelech, Z. Meng, S. Hong, Colloidal fouling in forward osmosis: role of reverse salt diffusion, J. Membr. Sci. 390–391 (2012) 277–284.
- [49] E.R. Cornelissen, D. Harmsen, K.F. de Korte, C.J. Ruiken, J.-j. Qin, H. Oo, L. P. Wessels, Membrane fouling and process performance of forward osmosis membranes on activated sludge, J. Membr. Sci. 319 (2008) 158–168.
- [50] C.Y. Tang, Q. She, W.C.L. Lay, R. Wang, A.G. Fane, Coupled effects of internal concentration polarization and fouling on flux behavior of forward osmosis membranes during humic acid filtration, J. Membr. Sci. 354 (2010) 123–133.
- [51] D.R. Paul, Reformulation of the solution-diffusion theory of reverse osmosis, J. Membr. Sci. 241 (2004) 371–386.
- [52] G.M. Geise, H.B. Park, A.C. Sagle, B.D. Freeman, J.E. McGrath, Water permeability and water/salt selectivity tradeoff in polymers for desalination, J. Membr. Sci. 369 (2011).
- [53] R.W. Holloway, A.E. Childress, K.E. Dennett, T.Y. Cath, Forward osmosis for concentration of centrate from anaerobic digester, Water Res. 41 (2007) 4005–4014.
- [54] J. Mallevialle, P.E. Odendaal, M.R. Wiesner, Water Treatment Membrane Processes, McGraw-Hill, USA, 1996.
- [55] C. Bellona, J.E. Drewes, G. Oelker, J. Luna, G. Filteau, G. Amy, Comparing nanofiltration and reverse osmosis for drining water augmentation, J. Am. Water Works Assoc. 100 (2008) 102–116.
- [56] J. Bohdziewicz, M. Bodzek, E. Wasik, The application of reverse osmosis and nanofiltration to the removal of nitrates from groundwater, Desalination 121 (1999) 139–147.
- [57] N.T. Hancock, W.A. Phillip, M. Elimelech, T.Y. Cath, Bidirectional permeation of electrolytes in osmotically driven membrane processes, Environ. Sci. Technol. 45 (2011) 10642–10651.
- [58] L. Paugam, S. Taha, G. Dorange, P. Joauen, F. Quemeneur, Mechanism of nitrate ions transfer in nanofiltration depending on pressure, ph, concentration and medium composition, J. Membr. Sci. 231 (2004) 37–46.
- [59] USEPA, National Primary Drinking Water Regulations, 2009.
- [60] J. Cho, G. Amy, J. Pellegrino, Membrane filtration of natural organic matter: initial comparison of rejection and flux decline characteristics with ultrafiltration and nanofiltration membranes, Water Res. 33 (1999) 2517–2526.
- [61] B.D. Coday, D.M. Heil, P. Xu, T.Y. Cath, Effects of transmembrane hydraulic pressure on performance of forward osmosis membranes, Environ. Sci. Technol. 47 (2013) 2386–2393.
- [62] C. Bellona, J.E. Drewes, P. Xu, G. Amy, Factors affecting the rejection of organic solutes during nf/ro treatment—a literature review, Water Res. 38 (2004) 2795–2809
- [63] R. Sheikholeslami, S. Zhou, Performance of ro membranes in silica bearing waters, Desalination 132 (2000) 337–344.
- [64] L.A. Hoover, W.A. Phillip, A. Tiraferri, N.Y. Yip, M. Elimelech, Forward with osmosis: emerging applications for greater sustainability, Environ. Sci. Technol. 45 (2011) 9824–9830.